



# Facile Synthesis, Diffused Reflectance Spectroscopy & Fluorescence Studies of $\text{Ni}_{0.5-x}\text{Mg}_{0.5}\text{Cu}_x\text{Fe}_2\text{O}_4$ Nanoparticles

Pradeep Chavan<sup>1</sup>

Received: 29 January 2021 / Accepted: 9 April 2021 / Published online: 23 April 2021

© The Author(s), under exclusive licence to Springer Science+Business Media, LLC, part of Springer Nature 2021

## Abstract

The present study focused on the structural, morphological, optical and fluorescence properties of  $\text{Ni}_{0.5-x}\text{Mg}_{0.5}\text{Cu}_x\text{Fe}_2\text{O}_4$  ( $x = 0.0, 0.1, 0.3$  and  $0.5$ ) nanoparticles synthesized by using auto combustion technique. The structural formation of the ferrite nanoparticles were confirmed by FTIR spectroscopic study. From FTIR spectra of the synthesized ferrite nanoparticles, metal ions are situated in two different sub lattices i.e. tetrahedral (A-site) and octahedral (B-site) in ferrites. The surface morphology and grain size of Cu substituted Ni-Mg ferrite nanoparticles were estimated from the micrographs of atomic force microscopy (AFM); the maximum grain size 54.69 nm was obtained. Spectra of UV-Visible absorption of the synthesized ferrite nanoparticles were carried-out by using UV-Vis spectrophotometry; the maximum absorption was observed at 418 nm. The energy band gap of ferrite nanoparticles has been estimated using UV-Vis absorption spectra; the energy band gap 3.50 eV was obtained. From the fluorescence emission spectra of the synthesized ferrite nanoparticles, ferrite samples emit red colour in the region of 680 nm.

**Keywords** Auto combustion technique · Ferrite nanoparticles · FTIR · UV-Visible · Fluorescence and energy band gap

## Introduction

Current advances in the field of material science enabled the community of research scientists to prepare and test the nano-scaled materials with different sizes, shapes and composition in favour of their miscellaneous applications [1]. The ferrite nanoparticles with spinel structure play extensively an important role in the development of fundamental research in technological applications owing to their distinctive structural, electrical, optical and fluorescence properties. Synthesis of ferrite nanoparticles and study of their physical properties is the significant part of research in the present decade. The use of appropriate preparation technique and proper analysis of several physical properties by using various characterization techniques can lead to the application of ferrite nanoparticles in various electronic technology and devices [2]. Thus, ferrites at the nano-scale acquire the noticeable physical and chemical properties than their bulk

forms. Therefore, these noticeable and extraordinary properties of the nanoparticles lead to the applicability of ferrites in diverse field ranging from electronics industry to the bio-medical field. Apart from its optical, magnetic and electric properties, ferrite materials find wide applications in heterogeneous catalysis and in sensor technology, microwave control components such as isolators, circulators, phase shifters, high density recording devices and magnetic technologies, etc. [3]. The consequence of molecular structure and motion of nanomaterials on the photochemical and photophysical properties of substituted ferrite nanoparticles have different modes of applications such as optoelectronics, optical data storage media and photonics, and also useful in thermal coagulation therapy were tumours are locally heated by the use of alternating magnetic field [4]. In recent years, ferrite nanomaterials attracted many researchers because of their various kinds of properties especially optical and fluorescence properties. Thus, the structural and optical properties of doped ferrite nanoparticles can be tuned by the type and amount of substituting elements chosen. Along with the nano-scaled materials, ferrite nanoparticles prove themselves as gifted materials for different practical device applications owing to their dual natured optical, electrical and magnetic properties [5].

✉ Pradeep Chavan  
cpajju@gmail.com

<sup>1</sup> Department of Studies in Physics, SB Arts & KCP Science College, Vijayapura 586103, Karnataka, India

In the present report, synthesis of  $\text{Ni}_{0.5-x}\text{Mg}_{0.5}\text{Cu}_x\text{Fe}_2\text{O}_4$  ferrite nanoparticles by using auto combustion method is carried out. We reported the study of spectroscopic properties like UV-Visible absorption spectroscopy, fluorescence emission spectroscopy and surface morphological studies of the synthesized ferrite nanoparticles.

## Experimental Details

Analytical reagent grade materials of high purity metal nitrates like  $\text{Ni}(\text{NO}_3)_2$ ,  $\text{Mg}(\text{NO}_3)_2$ ,  $\text{Cu}(\text{NO}_3)_2$  and  $\text{Fe}(\text{NO}_3)_3$  are taken in a stoichiometric percentage and dissolved in 50 ml deionized water for standardized mixture. 10 % of PVA solution was mixed with hot sucrose solution and stirred on the magnetic stirrer for the clear solution. All the prepared solutions were mixed together and then heated on the magnetic stirrer at the appropriate temperature until  $\text{NO}_2$  vapours vanished completely and form gelatinous mixture. This mixture was heated on the gas burner until it burns like live charcoal undergoing corrosion reaction for the configuration of ferrite nanoparticles in powder form. The powder was presintered at  $600\text{ }^\circ\text{C}$  for 8 h in the muffle furnace and cooled to room temperature. 2 % of PVA was added to this powder which acts as a binding agent and then hard-pressed into the form of pellets using the hydraulic press of 5 tons/inch<sup>2</sup>. The pellets were final sintered at  $800\text{ }^\circ\text{C}$  for 10 h and furnace cooled to room temperature.

## Results and Discussion

### FTIR Spectroscopy

The victorious manufacture of spinel nature and the presence of supplementary functional entities in synthesized Cu substituted Ni-Mg ferrite samples were studied by the gifted FTIR (Fourier transform infrared spectroscopy). FTIR spectroscopy is an important tool to identify the stretching and bending vibrations of tetrahedral and octahedral complexes of ferrite nanoparticles. IR absorption bands are the common feature of spinel type ferrite materials. FTIR spectra of synthesized  $\text{Ni}_{0.5-x}\text{Mg}_{0.5}\text{Cu}_x\text{Fe}_2\text{O}_4$  ferrite nanoparticles were shown in Fig. 1. The spectra of transmittance with respect to wavenumber were recorded in the range from  $400\text{ cm}^{-1}$  to  $4000\text{ cm}^{-1}$ . The absorption spectra confirmed the phase formation of cubic spinel structure and also elucidate the positions of cations in the crystal structure with oxygen ions as well as their vibrational modes [6].

These IR absorption bands represent the various ordering positions and structural properties of ferrite nanoparticles. The metal cations present in ferrite nanoparticles are situated in two different sub-lattices, i.e. tetrahedral (A-sites) sites and octahedral (B-sites) sites as stated by the oxygen ion nearest

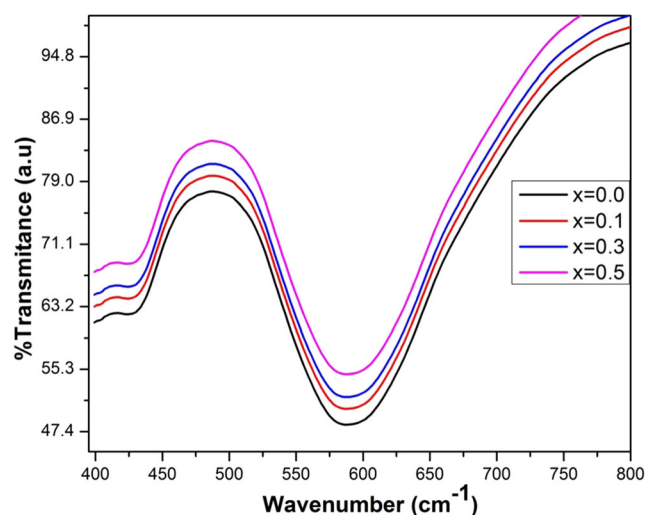


**Fig. 1** FTIR Spectra of  $\text{Ni}_{0.5-x}\text{Mg}_{0.5}\text{Cu}_x\text{Fe}_2\text{O}_4$  ferrite nanoparticles

neighbours in the geometric configuration [7]. The sample shows two prominent absorption bands  $\nu_1$  and  $\nu_2$  in the range of  $590\text{ cm}^{-1}$  and  $428\text{ cm}^{-1}$  respectively. The absorption band around  $590\text{ cm}^{-1}$  ( $\nu_1$ ) corresponds to intrinsic stretching vibration of metal cations at the tetrahedral site, while the band around  $428\text{ cm}^{-1}$  ( $\nu_2$ ) corresponds to metal cations at the octahedral sites [8] (Table 1).

Thus, the position of absorption bands  $\nu_1$  and  $\nu_2$  are expected at around  $600\text{ cm}^{-1}$  and  $400\text{ cm}^{-1}$  due to the difference between  $\text{Fe}^{3+}\text{-O}^{2-}$  distance of A–B site. Therefore, the band frequency  $\nu_2$  is less compared to the  $\nu_1$  band; it was due to the fact that dimension of A-site is less compared with the dimension of B-site [9]. The absorption band  $\nu_2$  is shifted slightly to higher frequency side because of the addition of  $\text{Cu}^{2+}$  ions and attributed to the increasing in bond length of B-site. This suggests that  $\text{Cu}^{2+}$  ions occupied B-site. The presence of  $\text{Fe}^{2+}$  ions causes the splitting of absorption bands due to local lattice deformation caused by Jahn-Teller effect [10].

### Atomic Force Microscopy

Microscopic observations can be available for monitoring the variation in surface morphology and microstructure of ferrite nanoparticles. Surface morphology and grain size of  $\text{Ni}_{0.5-x}\text{Mg}_{0.5}\text{Cu}_x\text{Fe}_2\text{O}_4$  nanoparticles were studied. Nanosurf Easyscan2 software is a tool utilized to estimate the grain size directly from the scanned image of the samples. Surface of the sample was scanned in a raster pattern by noncontact mode using AFM shown in Fig. 2. The grain size of the synthesized  $\text{Ni}_{0.5-x}\text{Mg}_{0.5}\text{Cu}_x\text{Fe}_2\text{O}_4$  nanoparticles of about 54.69 nm was observed. It is to be noted that the grain size increases with increasing copper concentration in Ni-Mg ferrite nanoparticles; it was due to the grain growth and variation in ionic radii of the metal cations [11]. As the grains of ferrites grow larger,

**Table 1** FTIR absorption bands, UV-Vis absorption wavelength, energy band gap and fluorescence excitation wavelength of the Cu substituted Ni-Mg ferrite nanoparticles

x content	Absorption bands (cm <sup>-1</sup> )		Absorption wavelength (nm)	Energy band gap (eV)	Excitation wavelength (nm)
	$\nu_1$	$\nu_2$			
0.0	590	423	411	3.50	679
0.1	588	426	413	3.22	678
0.3	588	428	416	3.10	678
0.5	588	428	418	2.82	680

the grains boundary becomes more obvious and the pores escape from the grain along with grain boundaries easily. These results in most of the remnant pores remain in grain boundaries and grains grow to be denser and homogeneous. As a result, many pores become isolated from grain boundaries and diffusion distance between the pores and grain boundary becomes large [12].

### UV-Visible Absorption Spectroscopy

Semiconducting ferrite nanoparticles which have absorption coefficient ( $\alpha$ ) and energy band gap ( $E_g$ ) are the major optical features which specify the ability to use for optoelectronic applications. The absorption coefficient ( $\alpha$ ) near the band edge shows an exponential upon photon energy usually obeying the expression as follows [13],

$$(\alpha hv)^2 = A(hv - E_g)^m \tag{1}$$

where  $\alpha$  is the absorption coefficient,  $h$  is the Plank constant, and  $v$  is the frequency of the incident radiation,  $E_g$  is the optical energy band gap,  $m$  is the nature of transition band gap (i.e.  $m = 1/2$  for indirect and 2 for direct band gap materials),  $A$  is a constant of independent energy and  $hv$  is photon energy.

Copper substituted Ni-Mg ferrite nanoparticles were analysed by using diffused UV-Visible reflectance spectroscopy to study their optical properties. Figure 3a shows UV-Visible absorption spectra with respect to wavelength of Ni<sub>0.5-x</sub>Mg<sub>0.5</sub>Cu<sub>x</sub>Fe<sub>2</sub>O<sub>4</sub> ferrite nanoparticles and it shows a maximum wavelength at 418 nm. It is to be noted that absorbance of copper substituted Ni-Mg ferrite nanoparticles ranging from 200 to 450 nm indicating the absorption of band edge has been broadened to region of visible light [14]. The absorbance characteristics of the nanostructured materials depend upon the number of factors such as energy band gap and surface roughness. Generally, energy band gap refers to the energy (eV) difference between valence band and conduction band. If the valence band is full of electrons and the conduction band is empty, then electrons cannot flow inside the materials; however, if some electrons transfer from the valence band to the conduction band then current can flow throughout the material [15]. Therefore, the energy band gap is an important parameter that determines the electrical conductivity of the materials. Hence, energy band gap is defined as occurring at the intercept of the linear extrapolation with x-axis. The energy band gap of polycrystalline ferrites estimated using Tauc plot. The graph of  $(\alpha hv)^2$  versus  $hv$  was plotted for Ni<sub>0.5-x</sub>Mg<sub>0.5</sub>Cu<sub>x</sub>Fe<sub>2</sub>O<sub>4</sub> nanoparticles to estimate the value of energy band gap of the synthesized ferrite nanoparticles shown in Fig. 3b. The energy

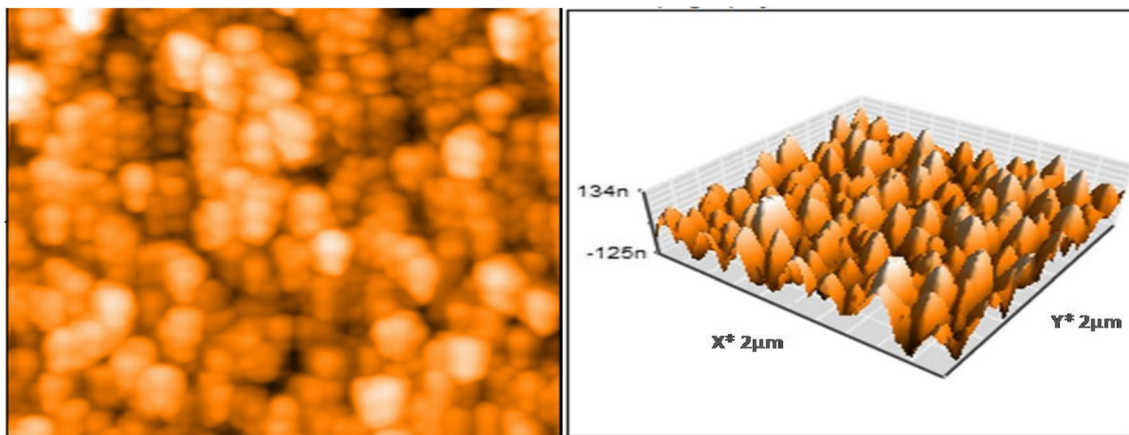


**Fig. 2** Surface morphological study of Ni<sub>0.5-x</sub>Mg<sub>0.5</sub>Cu<sub>x</sub>Fe<sub>2</sub>O<sub>4</sub> ferrite nanoparticles and 3D view of the ferrite samples

band gap was determined using Tauc [16] and Davis-Mott model [17] by extrapolating the linear portion of the plot to  $(\alpha h\nu)^2 = 0$  and we found the maximum energy band gap 3.50 eV. It is observed that the increase of energy band gap with increasing concentration of copper in Ni-Mg ferrite was due to increase in the lattice constant of the ferrite nanoparticles.

It is clear that all synthesized samples overcome with an absorption band in the whole range exhibited a fine absorption in the visible light region (200–450 nm). The absorption band observed at 418 nm is assigned to the characteristic absorption band of Cu-Ni-Mg ferrite nanoparticles. On substituting copper in Ni-Mg ferrites, the absorption band is shifted to higher wavelength which indicates a decrease in the energy band gap shown in Fig. 3b [18]. The fundamental absorption band that corresponds to excitation of an electron from valance band to conduction band can be used to determine the energy band gap of the synthesized ferrite nanoparticles.

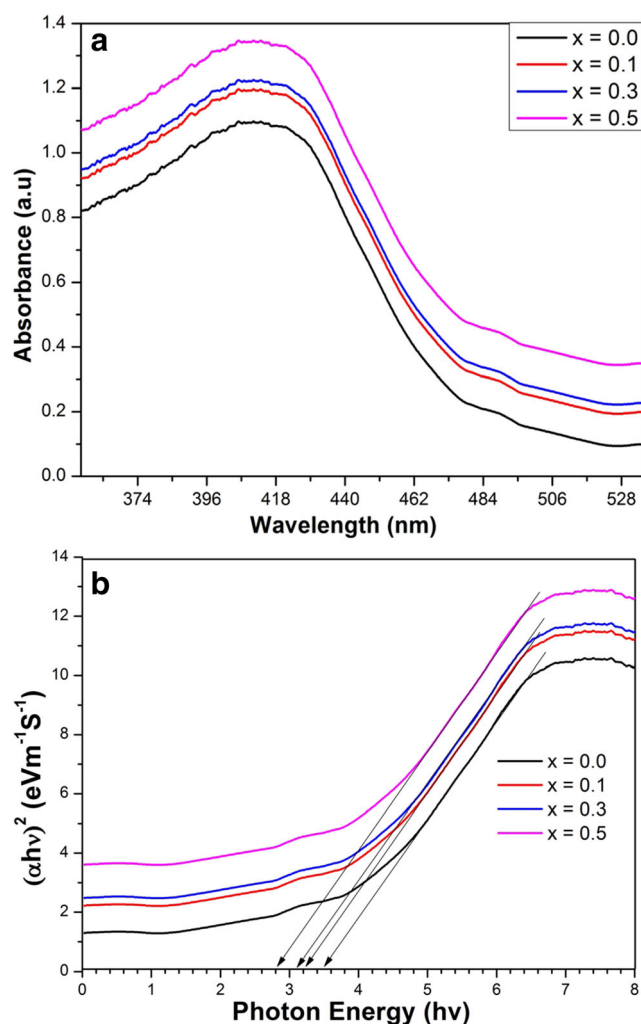


**Fig. 3** **a** UV-Visible absorption spectra of  $\text{Ni}_{0.5-x}\text{Mg}_{0.5}\text{Cu}_x\text{Fe}_2\text{O}_4$  ferrite nanoparticles. **b** Spectra of energy band gap of  $\text{Ni}_{0.5-x}\text{Mg}_{0.5}\text{Cu}_x\text{Fe}_2\text{O}_4$  ferrite nanoparticles

Thus, it is also observed that the decrease of energy band gap with respect to ferrite concentration was also be due to the sp-d exchange interaction between the localized d-electrons of  $\text{Cu}^{2+}$  ions and band electrons of Ni-Mg ferrite nanoparticles [19]. Thus the narrow energy band gap with Cu doping could be due to the formation of sub-bands in between the energy band gap and merging of their sub-bands with the conduction band to form a continuous band. Therefore, this decrease in the energy band gap with increasing Cu content in Ni-Mg ferrites which may be associated with several parameters including crystallite size, structural parameter, carrier concentration, presence of very small amount of impurities etc. [20].

## Fluorescence Studies

The fluorescence spectra of synthesized ferrite nanoparticles were recorded to investigate the luminescence properties and also to obtain the information on energy band gap with the relative energetic position of sub-band gap defect. The Fluorescence emission spectra of  $\text{Ni}_{0.5-x}\text{Mg}_{0.5}\text{Cu}_x\text{Fe}_2\text{O}_4$  nanoparticles were shown in Fig. 4. It is observed that for the excitation wavelength of 418 nm, the ferrite samples emit red colour in the region of 680 nm [21]. This property of emission was due to the  $\text{NO}_2$  and Nitrate groups present in ferrite nanoparticles. The cationic molecules weakly fluorescent in deionized water, when nitrates interact with the poly nucleotides then the fluorescence intensity increases [22]. The increasing copper concentration in  $\text{Ni}_{0.5-x}\text{Mg}_{0.5}\text{Cu}_x\text{Fe}_2\text{O}_4$  nanoparticles results in the shifting of peak towards red region ( $> 680$  nm) and fluorescence band became broaden can be ascribed to the formation of aggregated species [23].

Hence, the photo-induced electron transfer reaction is occurred mainly from a donor to an acceptor and it can be utilized for optical devices and optical storage applications etc.

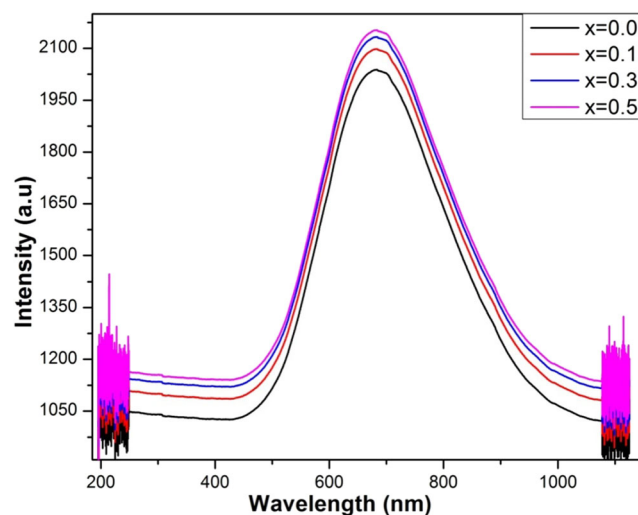


**Fig. 4** Fluorescence emission spectra of  $\text{Ni}_{0.5-x}\text{Mg}_{0.5}\text{Cu}_x\text{Fe}_2\text{O}_4$  ferrite nanoparticles

[24]. This fluorescent behaviour of  $\text{Ni}_{0.5-x}\text{Mg}_{0.5}\text{Cu}_x\text{Fe}_2\text{O}_4$  nanoparticles show gradually improved emission property which suggests that the enhancement of aggregation-induced fluorescence emission [25]. Thus, the emission characteristics of copper substituted Ni-Mg ferrite nanoparticles are governed by the defect controlled processes. It is also observed that doping of copper in Ni-Mg ferrites increases the fluorescence intensity with an increase in x values of copper. In spite of the fact that the defect controlled processes in all ferrite samples, the increase in the fluorescence intensity which was due to the increase in the distance between dopant (activator) and array [26]. Therefore, the defect center acts as trap levels and role of  $\text{Cu}^{2+}$  activators in increasing the intensity of fluorescence in the copper doped Ni-Mg ferrites play a dominant role in the emission processes [27].

## Conclusions

The Copper substituted Ni-Mg ferrite nanoparticles were synthesized by using auto combustion method. FTIR absorption spectra confirmed the formation of cubic spinel structure and also elucidate the positions of cations in the crystal structure with oxygen ions as well as their vibrational modes. The IR absorption bands represent the various ordering positions and structural properties for the different compositions of ferrites. The grain size of  $\text{Ni}_{0.5-x}\text{Mg}_{0.5}\text{Cu}_x\text{Fe}_2\text{O}_4$  nanoparticles was determined from AFM study; the maximum grain size 54.69 nm was obtained. All synthesized samples overcome with an absorption band in the whole range exhibited a fine absorption in the light region (200–450 nm). The absorption band observed at 418 nm is assigned to the characteristic absorption band of Cu-Ni-Mg ferrite nanoparticles. From the fluorescence emission spectroscopy of synthesized ferrite nanoparticles, the fluorescent behaviour of  $\text{Ni}_{0.5-x}\text{Mg}_{0.5}\text{Cu}_x\text{Fe}_2\text{O}_4$  nanoparticles show gradually improved emission property which suggests that the enhancement of aggregation-induced fluorescence emission.

**Author contributions** Not Applicable.

**Data availability** Data will be available on request.

**Code availability** Not Applicable.

## Declarations

**Conflicts of interest/Competing interests** Author hereby declare that the research article entitled "Facile Synthesis, Diffused Reflectance Spectroscopy & Fluorescence Studies of  $\text{Ni}_{0.5-x}\text{Mg}_{0.5}\text{Cu}_x\text{Fe}_2\text{O}_4$  Nanoparticles" have been submitted is not published elsewhere and not

yet communicated in any of the journals. Author declares that there is no conflict of interest.

**Ethics approval** Author approves the submission of research article to Journal of Fluorescence.

**Consent to participate** Author approves the consent to participate.

**Consent for publication** Author approves the consent for publication of this article into journal of fluorescence.

## References

1. Pankhurst QA, Connolly J, Jones SK, Dobson J (2003) Applications of magnetic nanoparticles in biomedicine. *J Phys D Appl Phys* 36:167
2. Kulikowski J (1990) Soft magnetic ferrites — Development or stagnation? *J Magn Magn Mater* 41:56
3. El Hiti MA (1999) AC electrical conductivity of Ni-Mg ferrites. *J Phys D Appl Phys* 29:501
4. Largeteau A, Reau JM, Raves J (1990) Dispersions diélectrique et d'impédance et énergies d'activation de céramiques à couches d'arrêt de type spinelle non stoechiométrique. *Phys Stat Sol A* 111:627
5. Abdeen AM (1999) Dielectric behaviour in Ni-Zn ferrites. *J Magn Magn Mater* 192:121
6. Koops CG (1951) On the dispersion of resistivity and dielectric constant of some semiconductors at audio frequencies. *Phys Rev* 83:121
7. Chavan P, Naik LR, Belavi PB, Chavan G, Ramesha CK, Kotnala RK (2017) Studies on electrical and magnetic properties of Mg-substituted nickel ferrites. *J Elect Mater* 46:188
8. Murthy VRK, Sobhanadri J (1976) Electrical conductivity of some nickel-zinc ferrites. *Phys Stat Sol A* 3:647
9. Naeem M, Shah NA, Gul IH, Maqsood A (2009) Structural, electrical and magnetic characterization of Ni-Mg spinel ferrites. *J Alloys Compd* 487:739
10. Gabal MA, Al Angari YM (2009) Effect of chromium ion substitution on the electromagnetic properties of nickel ferrite. *Mater Chem Phys* 118:153
11. Belavi PB, Chavan GN, Naik LR, Somashekar R, Kotnala RK (2012) Structural, electrical and magnetic properties of cadmium substituted nickel-copper ferrites. *Mater Chem Phys* 132:138
12. Shinde TJ, Gadkari AB, Vasambekar PN (2008) DC resistivity of Ni-Zn ferrites prepared by oxalate precipitation method. *Mater Chem Phys* 111:87
13. Waldron RD (1955) Infrared spectra of ferrites. *Phys Rev* 99:1727
14. Chavan P, Naik LR, Kotnala RK (2017) *J Magn Magn Mater* 433: 24
15. Costa ACFM, Kiminami RHGA, Santos PTA, Silva JF (2003)  $\text{ZnAl}_2\text{O}_4$  co-doped with Yb<sup>3+</sup>/Er<sup>3+</sup> prepared by combustion reaction: evaluation of photophysical properties. *Mater Sci* 48:172
16. Mahmoodi NM (2013) Magnetic ferrite nanoparticle-alginate composite: synthesis, characterization and binary system dye removal. *J Taiwan Inst Chem Eng* 44:322
17. Gaikwad RS, Chae S-Y, Mane RS, Han S-H, Joo O-S (2011) Structural properties of Cd-Co ferrites. *Int J Electrochem* 2011:1
18. Devan RS, Kolekar BKC (2006) Effect of cobalt substitution on the properties of nickel-copper ferrite. *J Phys Condens Matter* 18: 9809
19. Verwey EJW, de Boer F, van Santen JH (1948) Cation arrangement in spinels. *J Chem Phys* 16:1091

20. Pradeep Chavan LR, Naik PB, Belavi CG, Kotnala RK (2017) Synthesis of Bi<sup>3+</sup> substituted Ni-Cu ferrites and study of structural, electrical and magnetic properties. *J Alloy Compd* 694:607
21. Aisida SO et al (2020) Calcination effect on the photoluminescence, optical, structural, and magnetic properties of polyvinyl alcohol doped ZnFe<sub>2</sub>O<sub>4</sub> nanoparticles. *J Macromol Sci B*. <https://doi.org/10.1080/00222348.2020.1713519>
22. Wang S et al (2019) Effect of amorphous alumina and  $\alpha$ -alumina on optical, color, fluorescence properties and photocatalytic activity of the MnAl<sub>2</sub>O<sub>4</sub> spinel oxides. *J Light Elect Optic* 185:301
23. Debnath S, Das R (2020) Study of the optical properties of Zn doped Mn spinel ferrite nanocrystals shows multiple emission peaks in the visible range—a promising soft ferrite nanomaterial for deep blue LED. *J Mol Struct* 1199:127044
24. Chavan P, Naik LR (2017) Investigation of energy band gap and conduction mechanism of magnesium substituted nickel ferrite nanoparticles. *Phys Stat Solid A* 1700077:1
25. Thakur P et al (2019) Structural, morphological, magnetic and optical study of co-precipitated Nd<sup>3+</sup> doped Mn-Zn ferrite nanoparticles. *J Magn Magn Mater* 479:317
26. Talukdar S et al (2018) Facile surface modification of nickel ferrite nanoparticles for inherent multiple fluorescence and catalytic activities. *RSC Adv* 8:38
27. Shokri A et al (2018) The role of Co ion substitution in SnFe<sub>2</sub>O<sub>4</sub> spinel ferrite nanoparticles: study of structural, vibrational, magnetic and optical properties. *Ceram Int* 44:22092

**Publisher's note** Springer Nature remains neutral with regard to jurisdictional claims in published maps and institutional affiliations.